
Synthetic Site-Directed Ligands

A. B. Edmundson, J. N. Herron, K. R. Ely, X.-M. He, D. L. Harris and E. W. Voss

Phil. Trans. R. Soc. Lond. B 1989 **323**, 495-509

doi: 10.1098/rstb.1989.0027

Email alerting service

Receive free email alerts when new articles cite this article - sign up in the box at the top right-hand corner of the article or click [here](#)

To subscribe to *Phil. Trans. R. Soc. Lond. B* go to: <http://rstb.royalsocietypublishing.org/subscriptions>

Synthetic site-directed ligands

BY A. B. EDMUNDSON¹, J. N. HERRON¹, K. R. ELY¹, X.-M. HE¹,
D. L. HARRIS¹ AND E. W. VOSS, JR²

¹ Department of Biology, University of Utah, Salt Lake City, Utah 84112, U.S.A.

² Department of Microbiology, University of Illinois, Urbana-Champaign, Illinois 61081, U.S.A.

[Plate 1]

Complexes of nucleotides, peptides and aromatic hapten-like compounds with immunoglobulin fragments were studied by X-ray analysis. After tri- or hexanucleotides of deoxythymidylate were diffused into triclinic crystals of a Fab (BV04-01) with specificity for single-stranded DNA, extensive changes were detected throughout the structure of the protein. The Fab co-crystallized with a tri- or pentanucleotide in a different space group (monoclinic), an observation sometimes correlated with alterations in the structure of the 'native' protein. Structural analyses of the co-crystals are in progress for direct comparisons with the unliganded Fab.

In crystals of a human (Mcg) Bence-Jones dimer, synthetic opioid peptides, chemotactic peptides or dinitrophenyl (DNP) derivatives could be diffused into a large conical binding cavity. The conformations of both the ligand and the protein were usually altered during the binding process. At the base of the cavity tyrosine residues could be displaced like trap-doors to permit entry of some opioid peptides and DNP compounds into a deep binding pocket.

In co-crystals of the dimer and bis(DNP)lysine, two ligand molecules were bound in tandem, one in the main cavity and the second in the deep pocket. One ligand adopted an extended conformation, with the ϵ -DNP ring near the floor of the main cavity and the α -DNP group in solvent outside the binding site. There were no significant conformational changes in the protein. In contrast, the second ligand was very compact, with both DNP rings immersed in the deep pocket, and the binding site was expanded to accommodate the oversized ligand.

Peptides designed to be specific for the main cavity were incrementally constructed from minimal binding units by M. Geysen, G. Trippick, S. Rodda and their colleagues. A pentapeptide optimized for binding by this method was diffused into a crystal of the dimer and found by Fourier difference analysis to lodge exclusively in the main cavity as predicted.

Binding regions in the BV04-01 Fab and the Mcg dimer were markedly different in size and shape. The Fab had a groove-type site, in which a layer of sidechains acted like a false floor over regions analogous to the cavity and deep pocket of the Bence-Jones dimer.

INTRODUCTION

The crystal structure of the BV04-01 Fab has recently been determined at 2.7 Å† resolution (Herron *et al.* 1987; J. N. Herron, unpublished work). Consequently, we are just beginning to obtain binding patterns with site-directed nucleotides. In contrast, the structure of the second protein to be considered below (the Mcg Bence-Jones dimer) has been known for many years

$$\dagger 1 \text{ \AA} = 10^{-10} \text{ m} = 10^{-1} \text{ nm.}$$

[45]

(Schiffer *et al.* 1973; Edmundson *et al.* 1975). Extensive binding studies have been performed with the Mcg dimer by X-ray analysis after diffusion of potential ligands into crystals.

Both proteins were crystallized in 1.6–1.9 M ammonium sulphate, but the space groups (triclinic or trigonal) and crystal packing interactions were different. The Mcg dimer could be crystallized in an orthorhombic form in de-ionized water (Abola *et al.* 1980; Ely *et al.* 1983) but ammonium sulphate was more favourable for binding experiments with ligands such as nucleotides and peptides (contamination with bacteria or moulds was less frequent in ammonium sulphate).

As in the trigonal form of the Mcg dimer, the putative binding site of the BV04-01 Fab was accessible to compounds diffused through the crystal lattice. However, diffusion experiments proved more complicated than anticipated, and co-crystallization attempts were done in parallel. Other Fabs have been successfully co-crystallized with large antigens such as lysozyme (Amit *et al.* 1986; Sheriff *et al.* 1987) and influenza neuraminidase (Tulloch *et al.* 1986; Colman *et al.* 1987). For more direct comparisons with the liganded BV04-01 protein, murine Fabs from other anti-DNA antibodies have also been co-crystallized with oligonucleotides (Cygler *et al.* 1987; Anderson *et al.* 1988).

Apart from their inherent implications in the general field of molecular recognition, binding studies after diffusion or co-crystallization have been used to consider theories of 'lock and key' or 'induced fit' models of ligand-protein interactions. In early diffusion experiments, no significant conformational changes were observed in the binding of vitamin K₁OH to the human New Fab (Amzel *et al.* 1974) or in the binding of phosphorylcholine to the murine Fab McPC603 (Segal *et al.* 1974; see Padlan *et al.* 1985). Similar conclusions were reached in studies of lysozyme co-crystallized with the murine Fab D1.3 (Amit *et al.* 1986). Some conformational changes were noted in the epitope region of the antigen in a second complex of lysozyme and a murine Fab (HyHEL-5; Sheriff *et al.* 1987). Mutual conformational adjustments in the ligand and protein have been found in many examples of peptides diffused into crystals of the Mcg dimer (Edmundson *et al.* 1984, 1987; Edmundson & Ely 1985). Conformational changes in the antigens and antibodies were also believed to have occurred in the co-crystallization of influenza neuraminidases and murine Fabs (Colman *et al.* 1987).

In this paper we first describe preliminary attempts to assess the effects of ligand binding on the conformation of the BV04-01 Fab. Following this description there will be a discussion of past and present binding studies with the more primitive, but highly versatile Mcg dimer. Finally, we shall present experiments that partly reconcile the lock and key and induced fit models of ligand binding.

BINDING PROPERTIES OF BV04-01 IGG2B AUTOANTIBODY

To produce this monoclonal antibody, splenocytes from a female F₁ (New Zealand Black × New Zealand White) mouse with serum anti-DNA antibodies were chemically fused with a non-immunoglobulin-secreting myeloma cell line SP 2/0-Ag14 (Ballard *et al.* 1984; Ballard & Voss 1985). Such mice spontaneously develop a syndrome similar to human systemic lupus erythematosus.

The IgG2b (κ) autoantibody preferentially bound single-stranded DNA (e.g. thermally denatured calf thymus and plasmid DNA), with specificity for thymine bases (Ballard & Voss 1985). Binding of 5'-phosphorylated oligodeoxythymidylic acids was detectable after the chain

length exceeded five nucleotides. Relative binding constants for dephosphorylated oligodeoxythymidylic acids were augmented five- to tenfold when the size of the ligand was increased from ten to 18 nucleotides (Smith *et al.* 1989). Binding of synthetic nucleotides was characterized by an inverse temperature dependence between 2 and 40 °C. Variations in ionic strength did not appreciably affect the binding. For example, the binding decreased less than twofold as the concentrations of NaCl were increased from 0.15 to 1.5 M (Ballard & Voss 1985). These results suggested that the electrostatic interactions of the antibody with the phosphate groups of DNA did not play a major role in the stabilization of the ligand–protein complexes.

Crystal structure of the putative active site of the BV04-01 Fab

A stereo diagram of the C_α tracing of the BV04-01 Fab is shown in figure 1. The heavy chain is on the left and the light chain is on the right. The structure of the Fab is very extended. Pseudo-twofold axes of rotation between pairs of variable (V) domains and pairs of constant (C) domains were found to be confluent. In contrast, the corresponding angle ('elbow bend' angle) between the pseudodyads was 115° in the Mcg dimer. A large irregular groove between the tips of the V_H and V_L domains was designated as the probable binding site for single-stranded DNA (see open space to left of H31 label in figure 1). All three hypervariable loops of the light chain and the second and third hypervariable loops of the heavy chain were prominent in the formation of this groove.

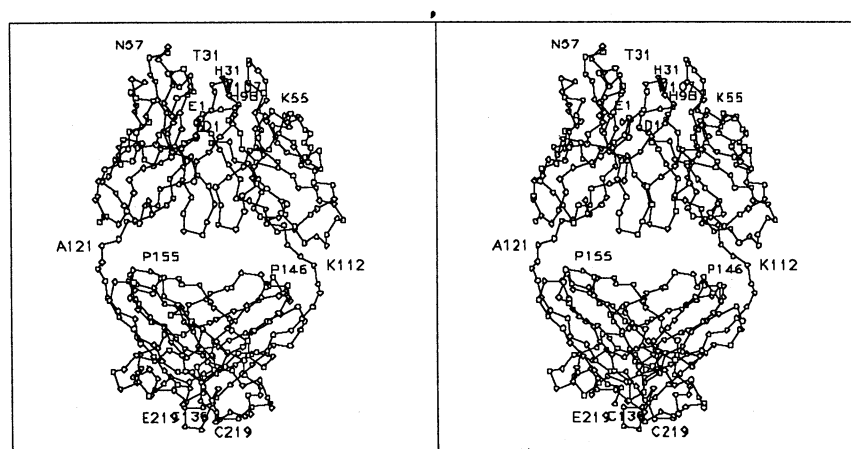


FIGURE 1. Stereo diagram of C_α tracing of the heavy (left) and light chains (right) of the BV04-01 Fab. The V domains are at the top and the C domains are at the bottom. Residues selected as general guides to the structure are labelled with their one-letter codes and sequence numbers. The putative DNA binding site is an irregular groove to the left of His 31 (light chain) at the top of the tracing. In the IgG2b subclass the interchain disulphide bond is formed by residue 136 of the heavy chain and the COOH-terminal residue (219) of the light chain (bottom of tracing).

In the electron-density map, Glu 219 was the last residue that could be identified in the heavy-chain moiety of the Fab (see E219 label in figure 1). It was therefore assumed that this was the site of papain cleavage of the BV04-01 antibody. As in other members of the IgG2b subclass, the interchain disulphide bond was formed between residues 136 (heavy chain) and 219, the COOH-terminal residue of the light chain (see bottom of model in figure 1).

Selected residues in the putative active site are presented in stereo in figure 2. One of the most interesting features of the structure was a cluster of sidechains acting like a false floor over a

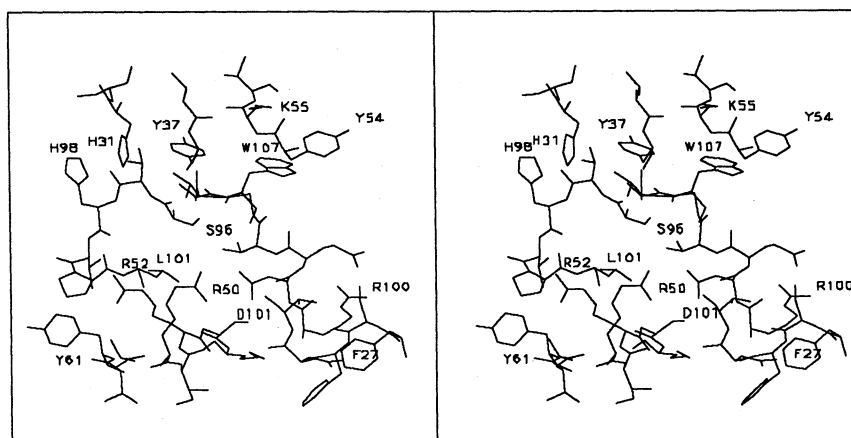


FIGURE 2. Stereo diagram of selected residues in the putative binding site of the BV04-01 Fab. Note the row of aromatic residues at the top of the site: His 98 and 31 and Tyr 37 and 54 are from the light chain and Trp 107 is a heavy-chain constituent. Access to a potential binding cavity analogous to that in the Mcg dimer (figure 4) is partly blocked by a cluster of sidechains: Ser 96 and Leu 101 of the light chain and Arg 50 and Asp 101 of the heavy chain. This is a good view of the ion pair formed by the Arg and Asp sidechains.

potential binding cavity of the type observed in the Mcg dimer (figure 4). This cluster consisted of Ser 96 and Leu 101 of the light chain, plus Arg 50 and Asp 101 of the heavy chain. The Arg and Asp sidechains formed a salt bridge across the entry to the cavity. The polypeptide backbone of the third hypervariable loop of the heavy chain, particularly around Ala 106, also partly blocked access to the cavity.

In view of the limited sensitivity of polynucleotide binding to changes in ionic strength, it was somewhat surprising to find so many positively charged residues in and around the groove (e.g. Lys 55, light chain, and Arg 50, 52 and 100, heavy chain in figure 2). In addition there were two His residues (31 and 98, light chain) that could have partial positive charges at pH values lower than that of the crystallization mixture (pH 7.3). Other aromatic sidechains lining the same part of the groove as His 31 were Tyr 37 and 54 (light chain) and Trp 107 (heavy chain).

X-ray analyses after diffusion of tri- and hexanucleotides of deoxythymidylate into crystals of BV04-01 Fab

Each nucleotide was added to the supernate over a crystal in a ratio two to five times the estimated molar quantity of protein. After soaking periods of two to seven days, the crystals were subjected to X-ray analysis. Diffraction data were collected to 2.7 Å resolution and subsequently compared with those for the unliganded Fab by Fourier difference analyses.

In the first experiment with the trinucleotide the crystal was cracked into unusable pieces within a week. If the soaking period was shortened to two days, it was possible to collect X-ray diffraction data. However, the difference Fourier map contained features of electron density corresponding to changes in many regions of the Fab molecule. In the putative binding site, there was a module of electron density possibly representing a ligand molecule and situated near Trp 107 of the heavy chain.

The presence of the hexanucleotide did not result in physical damage to the crystal. However, the changes in the protein molecule were as widely distributed as before. Although the largest feature in the difference map was again located in the vicinity of Trp 107, the structural perturbations elsewhere were too extensive to assign ligand positions with confidence.

Co-crystallization of the BV04-01 Fab and nucleotides of deoxythymidylate

Attempts were made to co-crystallize the Fab with tri-, tetra-, penta-, hexa- and octanucleotides in buffered ammonium sulphate with procedures initiated by Gibson *et al.* (1985). So far, co-crystals with tri- and pentanucleotides have been subjected to preliminary X-ray analyses (X.-M. He *et al.*, unpublished work). Both types crystallized in a space group (monoclinic) different from that (triclinic) of the unliganded protein. Using the atomic coordinates of the native BV04-01 Fab as a starting model, we obtained trial solutions of the structures of the two complexes (they are nearly isomorphous, except for the sizes of the ligands). The structures are currently being subjected to crystallographic refinement. It will be interesting to see if and how the structure of the protein has been changed in the binding of such relatively small ligands.

LIGAND BINDING IN THE MCG DIMER, A MODEL FOR A PRIMITIVE ANTIBODY

Description of a two-compartment binding system

The Mcg Bence-Jones dimer consists of two λ -type light chains with the same amino acid sequences but different conformations (Schiffer *et al.* 1973; Fett & Deutsch 1974; Edmundson *et al.* 1975). This dimer looks and acts like a Fab, with monomer 1 having the role of the heavy-chain analogue. We have therefore treated the dimer as a model for a primitive antibody and have explored the range of molecules that can be bound (Edmundson *et al.* 1974, 1984, 1987; Firca *et al.* 1978; Ely *et al.* 1978; Peabody *et al.* 1980; Edmundson & Ely 1985).

The V domain interface of the dimer is divided into two potential binding compartments: a large, conical main cavity and a smaller, ellipsoidal deep pocket below the floor of the cavity. There are only three charged side chains on the rim of the main cavity, one Asp and two Glu. Of the 21 sidechains lining the cavity, 12 are aromatic (eight Tyr, four Phe) and two additional aliphatic residues (Val) are also hydrophobic. However, it should be emphasized that the hydroxy groups of the eight Tyr and four Ser residues have often been utilized for hydrogen bonding with polar groups on otherwise hydrophobic ligands.

The floor of the main cavity is composed mainly of four aromatic residues (Tyr 38 and Phe 101 of each monomer), which are in Van der Waals contact in the native protein. Their sidechains (particularly those of Tyr 38) can be displaced to allow passage of some ligands into the deep pocket. This compartment is lined by only ten residues, including the four shared with the main cavity. The six additional residues include two Pro, two Tyr and two Gln.

Both compartments have proved to be malleable in the binding of ligands, such as 8-anilino-naphthalene-1-sulphonate (ANS) and menadione. ANS showed a preference for the main cavity and menadione lodged in the deep pocket (Edmundson *et al.* 1974, 1984). The binding activity of bis(ANS) was found to be increased 250-fold by the imposition of external pressure of 3 kbar[†] (Herron *et al.* 1985). After decompression the affinity remained ten times higher than its starting value. The binding pattern for menadione indicated that the deep pocket had expanded to accommodate the ligand, our first evidence for induced fit in the dimer (Edmundson *et al.* 1974).

[†]1 kbar = 10⁸ Pa.

Brief survey of binding properties of ligands used in previous studies

The general hydrophobic properties and large volume of the main cavity made it possible to explore the binding patterns of a wide variety of ligands. One of the most attractive side benefits was the opportunity to determine three-dimensional structures of bound ligands not currently amenable to X-ray analysis as isolated molecules.

The Mcg dimer was the only protein in our collection to produce sufficient numbers of crystals for screening of sizeable groups of related molecules. These groups included fluorescent compounds, *N*-formylated chemotactic peptides and opioid peptides (Edmundson *et al.* 1984, 1987; Edmundson & Ely 1985). Fluorescent compounds were very useful in monitoring the amount of space available for binding in the main cavity. Compounds increasing in size from ANS to fluorescein to bis(*N*-methyl)acridine (lucigenin) to dimers of carboxytetramethylrhodamine were diffused into trigonal crystals of the Mcg dimer. Different binding patterns were observed in each case, with the number of contacts progressively increasing until the main cavity was filled by the dimer of 6-carboxytetramethylrhodamine. The binding of the 6-isomer, in which the two carboxy groups were in *para* positions on the phenyl ring, could be discriminated from that of the 5-isomer, with the two carboxyl groups in *meta* positions. Hydrogen bonding with the hydroxy groups of Ser 36 and 91 (monomer 2) was sterically possible only when the carboxy groups were in *para* positions. As a consequence, the dimer of the 5-isomer occupied only the outer part of the main cavity and could be quantitatively removed by perfusion of the crystal with ammonium sulphate (the crystallizing medium). The 6-isomer could not be dislodged by the same procedure. In the binding of fluorescent ligands, particularly 6-carboxytetramethylrhodamine, the second and third hypervariable loops of the protein proved to be very flexible in expanding the combining site. Key Tyr and Phe sidechains were also highly mobile in the optimization of complementarity with the ligands. In this primitive system and with these synthetic ligands, the conformational adjustments appeared to be consistent with a limited neo-instructive theory of ligand binding.

In extending the studies to more flexible ligands, we fortunately selected two sets of hydrophobic peptides (chemotactic and opioid peptides) with biological activities mediated by receptors. Because selected members of both groups were bound to the Mcg dimer with high occupancy in feasibility trials, it was straightforward to design further experiments by following the leads in the extensive literature on receptor binding.

The stereochemical requirements for binding of *N*-formylated chemotactic peptides to the dimer were remarkably similar to those found in specific receptors on the plasma membranes of human and rabbit neutrophils (Schiffmann *et al.* 1975; Showell *et al.* 1976; Niedel *et al.* 1979; Freer *et al.* 1982; Marasco & Becker 1982). *N*-formylation was necessary in both Mcg and receptors, as evidenced by the failure of comparable peptides to bind if the α -amino groups were not derivatized. In each of five chemotactic peptides tested with Mcg, the *N*-formyl group was hydrogen bonded to the phenolic hydroxy group of Tyr 38, monomer 1. Methionine was optimal for binding in ligand position 1, although it could be replaced by norleucine (an unbranched residue) in both Mcg and receptors. In all cases the sidechain of Tyr 93 (monomer 2) was located in a new position, with electron density that was continuous with that of methionine in the difference Fourier map. The sidechain in ligand position 2 was less critical, providing it was bulky and hydrophobic (e.g. Leu, Met or Phe). The third ligand component could also be changed, but phenylalanine was the most favourable residue for binding.

N-f-tripeptides filled the main cavity and adopted wedge-shaped conformations that simulated the topography of the binding site. Unlike receptors, the Mcg dimer would not bind the tetrapeptide *N*-f-Met-Leu-Phe-Lys, presumably because the Lys sidechain could not be accommodated in the space between protein molecules in the crystal lattice. In analogy with the binding of fluorescent compounds, the outer protein loops were displaced to expand the site and the aromatic side chains were shifted to improve the complementarity with the ligand.

There was one unusual binding event worthy of mention. For *N*-f-Met-Trp, the *N*-formyl group and Met sidechain were in positions similar to those observed for other peptides in the series. However, the peptide bond between the Met and Trp was in the energetically less favourable *cis* configuration. With tripeptides it was possible that the comparable peptide bond had partial *cis* character, because neither a *cis* nor *trans* configuration was fully compatible with the electron density. However, additional interactions with the protein apparently prevented complete conversion of the peptide bond geometry to the *cis* form.

Inclusion of the opioid peptides in the binding studies added levels of complexity not encountered with either the chemotactic peptides or the fluorescent compounds. Collectively, the opioid peptides occupied sites encompassing all of the available space in the main cavity and deep pocket, as well as the external surfaces around the entrance to the cavity. In an extended conformation the pentapeptide [Met]enkephalin (Tyr-Gly-Gly-Phe-Met) could be accommodated inside the V domain interface, with the tyrosine sidechain in the deep pocket and the methionine residue at the entrance of the cavity. If Gly 2 was replaced by D-Ala, Tyr alone entered the cavity and the four remaining residues were found on the external surfaces. Again the structural features required for the binding of enkephalins and casomorphins to receptors were also important for interactions with the Mcg dimer (Snyder *et al.* 1974; Hughes *et al.* 1975; Goldstein 1976; Hambrook *et al.* 1976; Kosterlitz & Hughes 1978; Guillemin 1978; Terenius 1978; Henschen *et al.* 1979; Miller & Cuatrecasas 1979; Rossier *et al.* 1980; Morley 1980; Brantl *et al.* 1981; Hughes 1983). In both Mcg and opioid receptors, NH₂-terminal Tyr was necessary, but not sufficient for binding. For example, the peptides Gly-Gly-Phe-Met and Tyr-Gly-Gly failed to bind in the Mcg dimer. An (Arg 6, Phe 7) heptapeptide extension of [Met]enkephalin penetrated into the deep pocket and assumed an extended conformation in the main cavity like that of the pentapeptide. The last two residues of this peptide were flattened against the external surfaces. For as yet unknown reasons [Leu]enkephalin, with Leu substituted for Met, was restricted to the main cavity. The Tyr sidechain occupied a position at the junction between the cavity and the pocket and the peptide chain turned abruptly at Gly 3 at the entrance to the cavity. The last two residues interacted with external substituents of monomer 1.

As in [Met]enkephalin, the Tyr side chain of β -casomorphin-7 (Tyr-Pro-Phe-Pro-Gly-Pro-Ile) entered the deep pocket. The remainder of the peptide traversed the main cavity in as extended a conformation as possible with proline residues in positions 2 and 4. Pro 6 and Ile 7 were outside the cavity and not subject to any binding restrictions. Shorter peptides (e.g. β -casomorphins 4 and 5 and their variants) were bound in the main cavity, again with the tyrosine residues at the border between the cavity and pocket. As in the enkephalins, Tyr was dominant with respect to intermolecular contacts with the protein.

[Met]enkephalin, which was considered a high-occupancy, low-affinity ligand, could be quantitatively removed by perfusion of the crystal for two days. The β -casomorphins were also bound with high relative occupancies. In contrast to [Met]enkephalin, however, only about

half of β -casomorphin 7 could be washed out of the crystal in two days. On complete removal there was an unexpected hysteresis effect in which the walls of the deep pocket were permanently distorted.

Mutual displays of conformational flexibility of ligand and protein were major characteristics of the binding of opioid peptides. Changes were most severe when ligands such as [Met]enkephalin and β -casomorphin 7 spanned the main cavity and deep pocket. Aromatic sidechains along the entire path of each ligand were usually displaced and then rearranged to conform closely to the contours of the ligand. Even the relatively small peptide β -casomorphin 4 displaced six aromatic sidechains in the main cavity (Tyr 34, 38 and 93 of monomer 1; Tyr 34 and 38 and Phe 99 of monomer 2). After adjustments this peptide, like most of the others, appeared to be moulded to the internal image of the binding site.

Binding of bis(DNP)lysine in solution

By equilibrium dialysis in dilute aqueous buffers at pH 6.2, Peabody *et al.* (1980) found that one molecule of bis(DNP)lysine was bound to the Mcg dimer with an average association constant of $1.3 \times 10^5 \text{ M}^{-1}$. If slightly perturbed, the dimer could be converted into a molecular species binding two molecules of ligand with association constants of $2.3 \times 10^4 \text{ M}^{-1}$. The Scatchard plot was linear, an indication that the two ligand molecules were lodged in quasi-equivalent sites. It was assumed that one molecule interacted primarily with monomer 1 whereas the second associated with monomer 2. There were several ways to enhance the conversion to the divalent binding form, one simply involving exposure to a twofold molar excess of ligand for 24 h (Firca *et al.* 1978). After the ligand was quantitatively removed by dialysis, the protein only crystallized in an aberrant needle form (Ely *et al.* 1978) and gave abnormal aromatic circular dichroism (CD) spectra (K. J. Dorrington, in Firca *et al.* (1978)). When the interchain disulphide bond (70 Å away from the ligand binding site) was cleaved and allowed to reoxidize slowly, the dimer produced barrel-shaped trigonal crystals and aromatic CD spectra characteristic of the native protein (Ely *et al.* 1978). Moreover, the dimer reverted to a univalent binder of bis(DNP)lysine (Peabody *et al.* 1980). These experiments provided our first evidence that ligand binding was accompanied by allosteric changes in distal parts of the molecule. It was encouraging that these changes could be reversed, because we could now apply the same method to renature the protein after the binding of other ligands or after experiments with the protein in acidic solutions.

Binding of bis(DNP)lysine by diffusion into crystals

In trigonal crystals key residues for the binding of DNP compounds were first identified by affinity labelling with 1-fluoro-5-iodo-2,4-dinitrobenzene (Edmundson *et al.* 1974). After diffusion of stoichiometric amounts (2 moles per mole of protein) of this compound into a crystal, Tyr 34 and 38 of monomer 2 were the only residues found to be labelled by difference Fourier analysis. When bis(DNP)lysine was diffused into a crystal, the α -DNP ring was located near Tyr 34 of monomer 2 and the ϵ -DNP group was near the bottom of the main cavity and extended toward Tyr 38. The bias toward monomer 2 was mainly attributable to crystal-packing interactions that partly blocked access to Tyr 34 of monomer 1.

Ligand binding was accompanied by significant conformational changes in monomer 2 constituents close to the entrance of the cavity (especially Tyr 34) and in both monomers in the more confined space near the floor of the cavity.

Displacements of the sidechains at the base were probably correlated with the appearance of the ligand in the deep pocket. When the occupancy in the pocket reached about 20% of that in the main cavity, the crystal began to crack. Disintegration was progressive, although collection of X-ray data was possible until the occupancies in both binding sites were about 60% of the theoretical limits. Attempts to remove the ligands by perfusion of the crystal for two days with crystallization media (buffered ammonium sulphate) were ineffective, as monitored by X-ray analysis of the crystal. However, the ligand in the deep pocket could be displaced to the extent of about 85% by perfusion for a week with volumes of ammonium sulphate greater than 10^{10} times the estimated volume of the crystal. The occupancy in the main cavity actually increased by 22% during this period, presumably at the expense of the ligand diffusing out of the deep pocket.

This observed tenacity was seemingly at odds with the solution data, which indicated facile dissociation and a relatively modest affinity constant of *ca.* 10^5 M^{-1} for the binding of one ligand molecule.

Co-crystallization of bis(DNP)lysine and the Mcg dimer

Plausible explanations for many of these observations were suggested by the structural features of the ligand–protein complex in trigonal co-crystals (produced in ammonium sulphate). These crystals were isomorphous with those of the native protein, except of course for the presence of the ligands (Edmundson *et al.*, unpublished work). The structure of the complex was solved by difference Fourier analysis and then was crystallographically refined at 3.5 Å resolution.

Binding patterns in the co-crystals are depicted in figure 3 and figure 4, plate 1. The cage electron density corresponding to the ligands after refinement of the structure of the complex is displayed in figure 3. A schematic drawing of the binding region of the dimer is shown in profile in figure 4*a*, with a ligand model superimposed in its approximate orientation in the main cavity. A surface dot representation (Connolly 1983) of the ligands in their binding sites is presented in figure 4*b*.

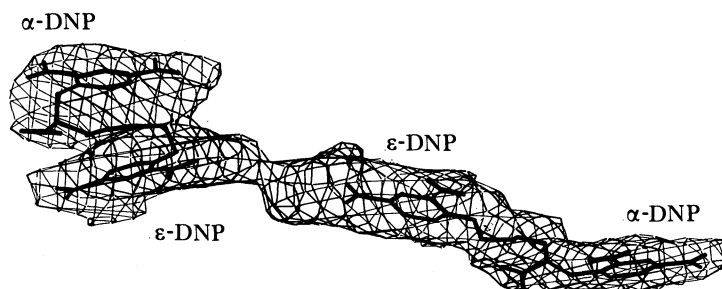


FIGURE 3. Three-dimensional 'cage' electron density corresponding to the two molecules of bis(DNP)lysine bound in tandem in the main cavity and deep pocket of the Mcg dimer. This electron density was obtained in a difference Fourier map after crystallographic refinement of the ligand–protein complex in co-crystals. Skeletal models of the two ligands are superimposed on the electron density.

These figures show that two ligand molecules were bound in tandem, one in the main cavity and one in the deep pocket. The outer ligand was directed down the middle of the main cavity, with a slight bias toward monomer 1. The molecule was almost fully extended, with a ring to ring distance of 11.2 Å. Contrary to our expectations from the diffusion experiments, only one DNP ring entered the cavity. The ε-DNP group was flanked by the two Phe 99 sidechains, and

also was stabilized by interactions with Tyr 93, monomer 1, and Tyr 38, monomer 2. There were only 25 interactions less than 4 Å with the protein, and these were associated exclusively with the ε-DNP ring. The α-carboxy group was exposed to solvent at the entrance and the α-DNP group was located outside the cavity.

In the deep pocket the ligand adopted a very compact structure, with both DNP rings immersed and only separated by 7.2 Å. The ε-DNP group was wedged into the space near the entrance of the pocket, whereas the α-DNP ring was situated near the exit. The 4-nitro group of the latter was in contact with the Gln 40 sidechains of both monomers. The α-carboxy group appeared to be buried in a slot between the β-carbon atoms of Tyr 38 and 89 of monomer 1. However, the packing of ligand and protein was too tight in this region to determine whether there were any interactions to compensate for the putative charge on the carboxy group. In contrast to the outer ligand, the molecule in the deep pocket was in very close contact with the protein (there were 186 interatomic distances less than 4 Å between ligand and protein).

Ligand binding was accompanied by few significant conformational changes in the main cavity; in fact, the delicate placement of the ligand was consistent with a paucity of collisions. As expected, the residues important for crystal packing interactions (e.g. Tyr 34, monomer 1) were not involved in the binding of ligand in co-crystals.

The situation was quite different in the deep pocket, which had expanded to accommodate the oversized ligand. Coupled sets of negative and positive contours of electron density in the difference map indicated that the backbone and sidechains of residues 45–47 in both monomers were displaced by 1–2 Å. Smaller dislocations of the polypeptide chains occurred in positions 38 and 89 of monomer 1 and 38, 39, 40 and 101 of monomer 2. Significant shifts were also noted in the sidechains of Tyr 38 and 89, Gln 40 and Phe 101 of both monomers.

Bis(DNP)lysine was readily removed from the main cavity in co-crystals, but the occupancy of the ligand in the deep pocket was not decreased even after ten days of perfusion with crystallizing media. These results suggest that the 'co-crystal type' of binding in the main cavity was similar to that occurring in solution, but substantially different from the behaviour of bis(DNP)lysine when diffused into pre-existing crystals.

If the binding energy was primarily dependent on the contributions of only one of the two DNP groups, we might have expected the relatively low affinity constant obtained in solution by equilibrium dialysis methods and the relative ease with which bis(DNP)lysine could be released from co-crystals by perfusion. Conversely, with both rings in intimate contact with the protein inside the main cavity, it was not surprising to find that the binding was practically irreversible in the diffusion experiments. Because of restricted access to part of the cavity in the crystal lattice, the binding patterns in trigonal crystals could not be used as direct models for the solution state in which two molecules of bis(DNP)lysine occupied quasi-equivalent sites. However, the ease of dissociation by dialysis and the low affinity constants again suggest that only one DNP ring from each ligand was inserted into the main cavity. This suggestion was supported by model-building exercises, which indicated that it would be sterically difficult for two bis(DNP)lysine molecules to be completely immersed in the main cavity in symmetry-related sites.

Predictions based on the dominant contributions of a single DNP ring in solution were tested with ε-DNP Lys as ligand. The average association constant for this compound was found by equilibrium dialysis to be $2.6 \times 10^4 \text{ M}^{-1}$, a value less than one order of magnitude lower than that of bis(DNP)lysine (this value was kindly provided by S. Nichols). In a parallel project at

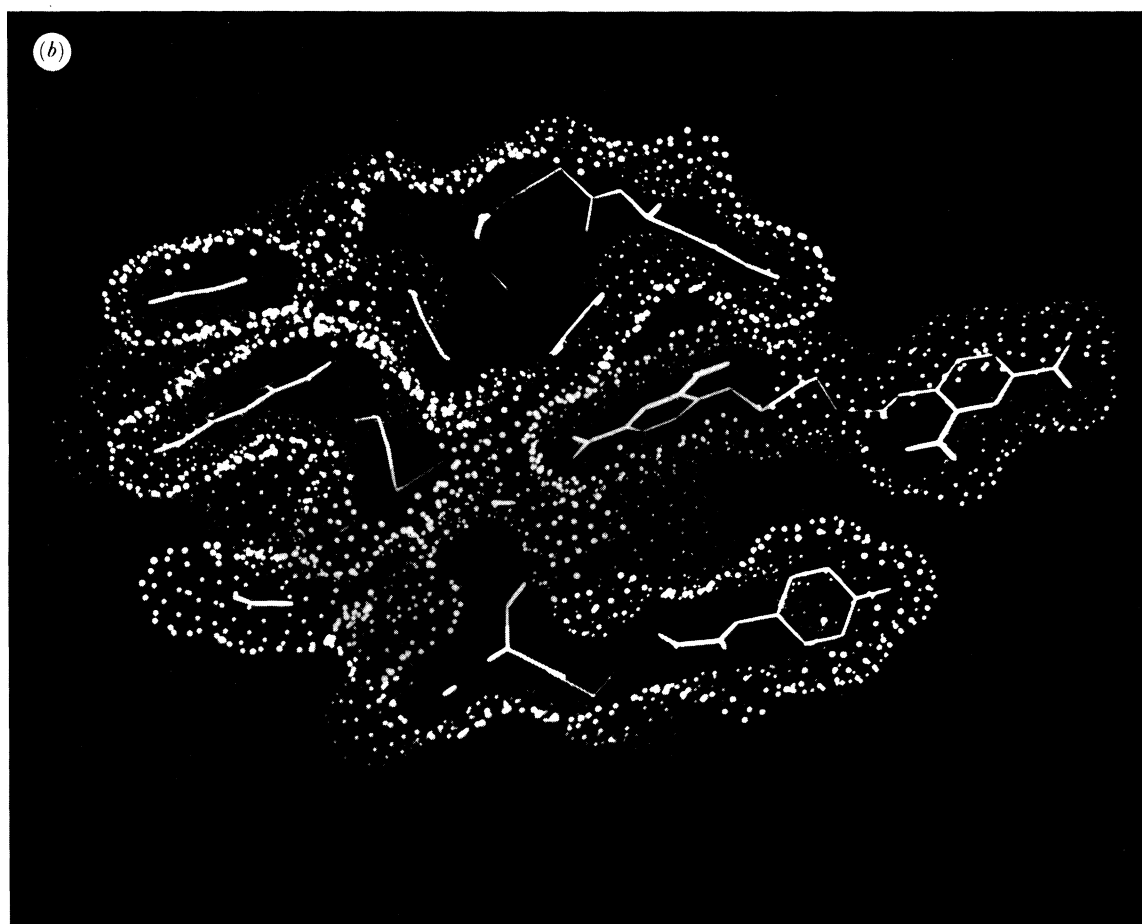
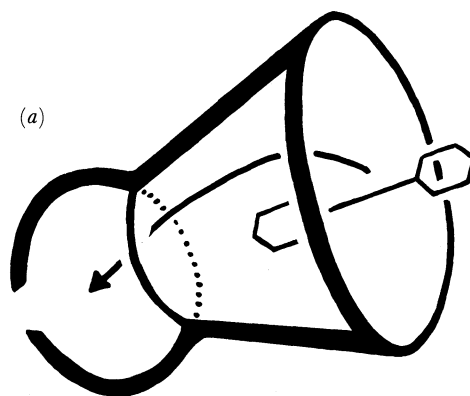


FIGURE 4. (a) Schematic view of the conical main cavity (right) and the ellipsoidal deep pocket (left). A model of bis(DNP)lysine is drawn in the approximate orientation observed in co-crystals of the ligand and protein. The arrow indicates a possible path to the deep pocket. (Drawing by Kathryn Ely.) (b) Surface dot representation (Connolly 1983) of the two tandemly bound molecules of bis(DNP)lysine in the main cavity (right) and deep pocket (left). This cutaway view was photographed directly from the screen of an Evans & Sutherland PS300 colour graphics system. The ligand molecule on the right is almost fully extended, and only one DNP ring is located inside the main cavity. This bis(DNP)lysine on the left is very compact and is completely enclosed in the deep pocket.

(Facing p. 504)

the Commonwealth Serum Laboratories in Melbourne, Australia, DNP compounds were tethered to solid supports and assayed for binding to the Mcg dimer by the method of Geysen *et al.* (1987). The relative affinity of ϵ -DNP lysine for the dimer was 90% as great as that of bis(DNP)lysine. In these cases the results in solution were consistent with crystal diffusion studies, in which ϵ -DNP lysine and DNP Leu could be quantitatively removed from the main cavity by perfusion for two days (Edmundson *et al.* 1974).

The tenacious binding in the deep pocket in co-crystals led us to develop procedures for preparing similar complexes in solution. If the Mcg dimer was first exposed to large quantities of bis(DNP)lysine (5–10 moles per mole of protein), it was found by spectrophotometric techniques that $43 \pm 8\%$ of the ligand remained bound to the protein after exhaustive dialysis (16 days). We concluded that the ligands removed by dialysis had been located in the main cavity, whereas the firmly sequestered molecules were lodged in the deep pocket.

Thus in both solution and co-crystals, a flexible ligand formed at least two types of complexes with one malleable protein molecule. In co-crystals one extended ligand molecule assumed a conformation that closely matched an internal image in the main cavity and bound with moderate affinity mediated by interactions with only one of its two DNP rings. The second ligand in the same protein adopted a compact and convoluted conformation that depended on mutual adjustments with a small but expandable pocket. With more than seven times as many contacts with the protein, the second ligand bound with high affinity. In solution, the analogous ligand behaved like a virtually irreversible inclusion compound.

When diffused into a pre-existing crystal, the outer ligand adopted a linear but compressed conformation with both DNP rings enclosed within the main cavity. The protein was distorted and the ligand remained firmly bound after perfusion of the crystal. The second ligand was also difficult to dislodge, but eventually could be washed out of the deep pocket. A gradual increase in occupancy in this site was reflected in progressive physical deterioration of the crystal.

Collectively, the results suggest that the properties of co-crystals could be used to reconcile two current views of antigen–antibody interactions: lock and key versus induced-fit hypotheses. Binding in the main cavity proceeded with minimal perturbations of the types seen with the same ligand and protein in other environments. Conversely, binding in the deep pocket was associated with substantial changes in the shapes and sizes of both ligand and binding site.

BINDING OF A PEPTIDE DESIGNED FOR THE MCG DIMER

The Mcg dimer was systematically tested for binding activity against peptides coupled to solid supports (G. Tribbick, M. Geysen, T. Mason & A. Edmundson, unpublished work). After minimal binding units were identified, peptides incrementally increasing in affinity for the protein were synthesized by successive additions of amino acid residues. Both the sequence and combination of optical isomers were optimized for activity at each stage of the synthesis. Di-, tri-, tetra- and pentapeptides selected from this series were then synthesized in milligram quantities for diffusion into trigonal crystals of the dimer.

These studies are still in progress, but general trends are now evident. Peptides that had binding activity when tethered to rods also acted as ligands when diffused into crystals. As predicted, the peptides were accommodated exclusively in the main cavity. These findings provided further support for the applicability of the method of Geysen *et al.* (1987) for determining peptide specificity in immunoglobulin-binding sites.

The binding pattern for one of the most active peptide ligands is illustrated in figure 5. A skeletal model of the peptide in the conformation it adopted in the main cavity is shown in (a). The sequence of the peptide was *N*-acetyl-L-Gln-D-Phe-L-His-D-Pro- β -Ala. In the system of Geysen *et al.* (1987) the β -Ala residue would have been connected to a rod by a long hydrophobic spacer. The cage electron density corresponding to the peptide is co-displayed with the skeletal model in (b). In (c) this electron density feature is superposed on a skeletal model of the binding region to show the orientation of the peptide in the main cavity.

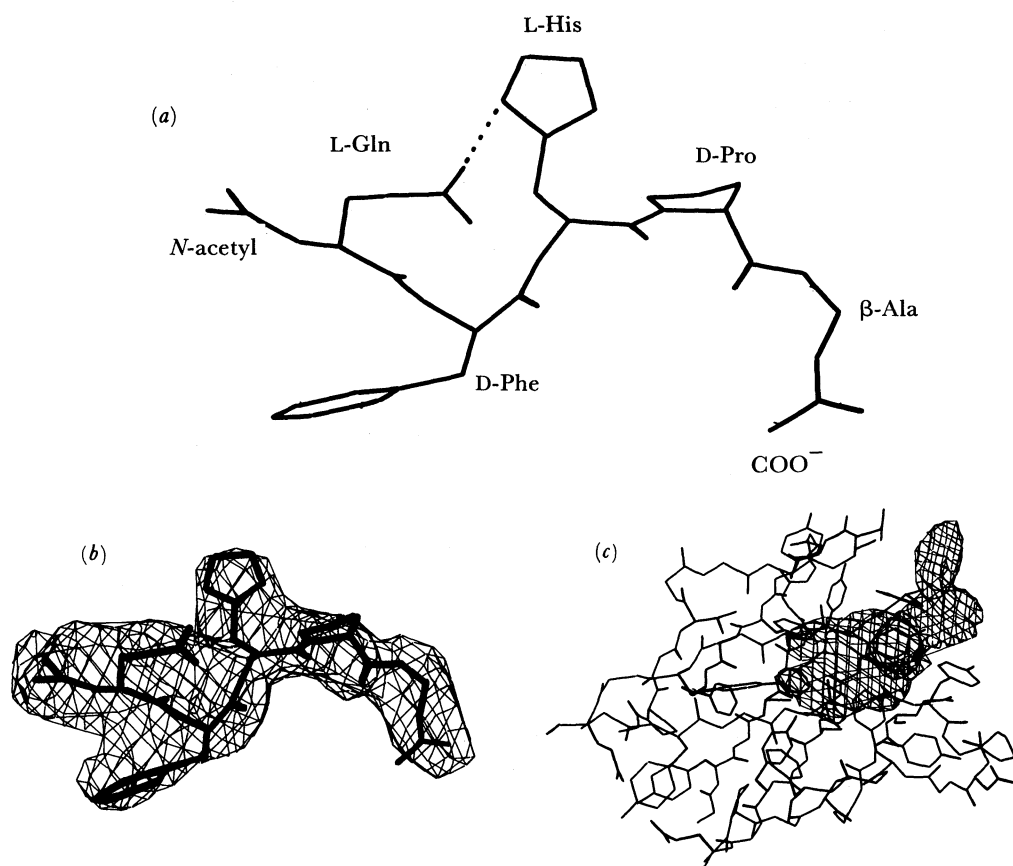


FIGURE 5. (a) Structure of a peptide as bound in the main cavity after diffusion into a crystal of the Mcg dimer. This peptide was constructed by incremental additions to minimal binding units by the method of Geysen *et al.* (1987). At each stage peptides were systematically tested for optimal binding to the Mcg dimer (see text). The dotted line between the side chains of Gln and His indicates that the two atoms are within hydrogen-bonding distance. (b) Cage electron density for the peptide in a 2.7 Å difference Fourier map calculated after crystallographic refinement of the ligand-protein complex. The model of the peptide is superimposed on the electron density. (c) Cage electron density co-displayed with a skeletal model of the Mcg main cavity and deep pocket to illustrate the general mode of binding of the peptide.

As expected, the *N*-acetyl group entered the cavity first. It was stabilized in a well-defined position by 12 contacts (less than 4 Å) with protein substituents. The carbonyl oxygen formed a hydrogen bond with the phenolic hydroxyl group of Tyr 38, monomer 2. The L-Gln residue was also stabilized in a fixed position. Of 20 contacts with the protein, all but four were with monomer 1 constituents, especially Phe 99 (11 contacts) and Tyr 93 (five contacts). D-Phe occupied a hydrophobic subsite and made an exceptional number (36) of contacts with the protein, again mainly with monomer 1 components (32 contacts). Six protein residues were

involved in these contacts, especially Val 48, Tyr 34 and Tyr 51 of monomer 1. All four contacts with monomer 2 were provided by Phe 99. In contrast, interactions with L-His were limited to monomer 2 components (11 contacts), primarily Tyr 34 (seven contacts) and Glu 52 (three contacts). D-Pro and β -alanine were not in direct contact with the protein.

It was curious that the minimal binding unit for this peptide was *N*-acetyl-L-His-D-Pro, when 70% of the contacts in the optimized pentapeptide were furnished by L-Gln and D-Phe. In the Mcg IgG1 immunoglobulin, with the same light-chain sequence as in the Mcg Bence-Jones dimer, the basic binding unit was *N*-acetyl-L-Gln-D-Phe (Geysen *et al.*, unpublished work). The structure presented in figure 5 suggests why the combination of L-His-D-Pro and L-Gln-D-Phe was favoured at the tetrapeptide level. The Gln sidechain extended toward the entrance of the cavity and the amide group formed a hydrogen bond with the imidazole group of the histidine residue.

These structural features indicated how Gln could act as an antigenic determinant even in a hydrophobic binding cavity. Methylene groups of the chain could interact with hydrophobic groups on the protein (in Mcg it was mainly Phe 99). Compensation for the amide group could be achieved internally within the epitope (as in this case) or externally by hydrogen bonding with a Tyr or Ser hydroxy group inside the cavity. There were other precedents for such interactions in Mcg. In an otherwise hydrophobic environment, for example, the amide groups of the two Gln 40 sidechains of monomers 1 and 2 formed close contacts with each other at the exit of the deep pocket.

One of the objectives of this collaborative study was to find a peptide that would simulate an epitope on a protein. The peptide in figure 5 filled several criteria favourable for such simulation. Like a protein loop that would be restricted by its neighbouring segments, a substantial fraction of the peptide did not penetrate very deeply into the main cavity. For example, the Pro residue was located at the entrance of the cavity and the COOH-terminal β -Ala was outside the rim in bulk solvent. In its bound form, the peptide was internally stabilized by a hydrogen bond between the sidechains of its Gln and His residues, again in analogy with a possible protein loop.

The shape of the peptide was well matched by the topography of the cavity and there were many (80) close contacts. Moreover, the conformational changes in the protein were moderate in comparison with those observed in the binding of the chemotactic and opioid peptides. The walls of the cavity were not expanded and the movements of contact residues generally involved only small rotations of aromatic rings and displacements of sidechains by less than 1 Å. These findings indicate that rather sophisticated ligands can be designed to be accommodated without major distortions of the binding site.

We are deeply grateful to Mario Geysen, Gordon Tribbick, Stuart Rodda, Tom Mason and their colleagues in Melbourne for the design, testing and synthesis of the peptide discussed in the last section of this paper. We also thank the Melbourne group for many stimulating discussions, Barbara Staker for her artwork, Brad Nelson for his photography and Judy Baker for preparing the manuscript for publication.

REFERENCES

- Abola, E. E., Ely, K. R. & Edmundson, A. B. 1980 Marked structural differences of the Mcg Bence-Jones dimer in two crystal systems. *Biochemistry, Wash.* **19**, 432–439.
- Amit, A. G., Mariuzza, R. A., Phillips, S. E. V. & Poljak, R. J. 1986 Three-dimensional structure of an antigen–antibody complex at 2.8 Å resolution. *Science, Wash.* **233**, 747–753.
- Amzel, L. M., Poljak, R. J., Saul, F., Varga, J. M. & Richards, F. F. 1974 The three-dimensional structure of a combining-region–ligand complex of immunoglobulin New at 3.5 Å resolution. *Proc. natn. Acad. Sci. U.S.A.* **71**, 1427–1430.
- Anderson, W. F., Cygler, M., Braun, R. P. & Lee, J. S. 1988 Antibodies to DNA. *BioEssays* **8**, 69–74.
- Ballard, D. W., Lynn, S. P., Gardner, J. E. & Voss, E. W. Jr 1984 Specificity and kinetics defining the interaction between a murine monoclonal autoantibody and DNA. *J. biol. Chem.* **259**, 3492–3498.
- Ballard, D. W. & Voss, E. W. Jr 1985 Base specificity and idiotype of anti-DNA autoantibodies with synthetic nucleic acids. *J. Immunol.* **135**, 3372–3386.
- Brantl, V., Teschemacher, H., Blasig, J., Henschen, A. & Lottspeich, F. 1981 Opioid activities of β -casomorphins. *Life Sci.* **28**, 1903–1909.
- Colman, P. M., Laver, W. G., Varghese, J. N., Baker, A. T., Tulloch, P. A., Air, G. M. & Webster, R. G. 1987 Three-dimensional structure of a complex with influenza virus neuraminidase. *Nature, Lond.* **326**, 358–363.
- Connolly, M. L. 1983 Solvent-accessible surfaces of proteins and nucleic acids. *Science, Wash.* **221**, 709–713.
- Cygler, M., Boodhoo, A., Lee, J. S. & Anderson, W. F. 1987 Crystallization and structure determination of an autoimmune anti-poly(dt) immunoglobulin Fab fragment at 3.0 Å resolution. *J. biol. chem.* **262**, 643–648.
- Edmundson, A. B. & Ely, K. R. 1985 Binding of *N*-formylated chemotactic peptides in crystals of the Mcg light chain dimer: similarities with neutrophil receptors. *Molec. Immunol.* **22**, 463–475.
- Edmundson, A. B., Ely, K. R., Abola, E. E., Schiffer, M. & Panagiotopoulos, N. 1975 Rotational allomerism and divergent evolution of domains in immunoglobulin light chains. *Biochemistry, Wash.* **14**, 3953–3961.
- Edmundson, A. B., Ely, K. R., Girling, R. L., Abola, E. E., Schiffer, M., Westholm, F. A., Fausch, M. D. & Deutsch, H. F. 1974 Binding of 2,4-dinitrophenyl compounds and other small molecules to a crystalline λ -type Bence-Jones dimer. *Biochemistry, Wash.* **13**, 3816–3827.
- Edmundson, A. B., Ely, K. R. & Herron, J. N. 1984 A search for site-filling ligands in the Mcg Bence-Jones dimer: crystal-binding studies of fluorescent compounds. *Molec. Immunol.* **21**, 561–576.
- Edmundson, A. B., Ely, K. R., Herron, J. N. & Cheson, B. D. 1987 The binding of opioid peptides to the Mcg light chain dimer: flexible keys and adjustable locks. *Molec. Immunol.* **24**, 915–935.
- Ely, K. R., Firca, J. R., Williams, K. J., Abola, E. E., Fenton, J. M., Schiffer, M., Panagiotopoulos, N. C. & Edmundson, A. B. 1978 Crystal properties as indicators of conformational changes during ligand binding or interconversion of Mcg light chain isomers. *Biochemistry, Wash.* **17**, 158–167.
- Ely, K. R., Herron, J. N. & Edmundson, A. B. 1983 Three-dimensional structure of the orthorhombic form of the Mcg Bence-Jones dimer. *Prog. Immunol.* **5**, 61–66.
- Fett, J. W. & Deutsch, H. F. 1974 Primary structure of the Mcg chain. *Biochemistry, Wash.* **13**, 4102–4114.
- Firca, J. R., Ely, K. R., Kremser, P., Westholm, F. A., Dorrington, K. J. & Edmundson, A. B. 1978 Interconversion of conformational isomers of light chains in the Mcg immunoglobulins. *Biochemistry, Wash.* **17**, 148–158.
- Freer, R. J., Day, A. R., Muthukumaraswamy, N., Pinon, D., Wu, A., Showell, H. J. & Becker, E. L. 1982 Formyl peptide chemoattractants: a model of the receptor on rabbit neutrophils. *Biochemistry Wash.* **21**, 257–263.
- Geysen, H. M., Rodda, S. J., Mason, T. J., Tribbick, G. & Schoofs, P. G. 1987 Strategies for epitope analysis using peptide synthesis. *J. immunol. Meth.* **102**, 259–274.
- Gibson, A. L., Herron, J. N., Ballard, D. W., Voss, E. W. Jr, He, X. M., Patrick, V. A. & Edmundson, A. B. 1985 Crystallographic characterization of the Fab fragment of a monoclonal anti-ss-DNA antibody. *Molec. Immunol.* **22**, 499–502.
- Goldstein, A. 1976 Opioid peptides (endorphins) in pituitary and brain. *Science, Wash.* **193**, 1081–1086.
- Guillemín, R. 1978 Peptides in the brain: the new endocrinology of the neuron. *Science, Wash.* **202**, 390–402.
- Hambrook, J. M., Morgan, B. A., Rance, M. J. & Smith, C. F. C. 1976 Mode of deactivation of the enkephalins by rat and human plasma and rat brain homogenates. *Nature, Lond.* **262**, 782–783.
- Henschen, A., Lottspeich, F., Brantl, V. & Teschemacher, H. 1979 Novel opioid peptides derived from casein (β -casomorphins). *Hoppe-Seyler's Z. physiol. Chem.* **360**, 1217–1224.
- Herron, J. N., Ely, K. R. & Edmundson, A. B. 1985 Pressure-induced conformational changes in a human Bence-Jones protein (Mcg). *Biochemistry, Wash.* **24**, 3453–3459.
- Herron, J. N., He, X.-M., Gibson, A. L., Voss, E. W. Jr & Edmundson, A. B. 1987 Crystal structure of a murine Fab fragment with specificity for single-stranded DNA. *Fedn Proc. Fedn Am. Socs exp. Biol.* **46**, 1626.
- Hughes, J. 1983 Biogenesis, release and inactivation of enkephalins and dynorphins. *Br. med. Bull.* **39**, 17–24.
- Hughes, J. W., Smith, T., Kosterlitz, H. W., Fothergill, L. H., Morgan, B. A. & Morris, H. 1975 Identification of two related pentapeptides from the brain with potent opiate agonist activity. *Nature, Lond.* **258**, 577–579.

- Kosterlitz, H. W. & Hughes, J. 1978 Development of the concepts of opiate receptors and their ligands. *Adv. Biochem. Psychopharmac.* **18**, 31–44.
- Marasco, W. A. & Becker, E. L. 1982 Anti-idiotypic antibody against the formyl peptide chemotaxis receptor of the neutrophil. *J. Immunol.* **128**, 963–968.
- Miller, R. J. & Cuatrecasas, P. 1979 Enkephalins and endorphins. *Vitam. Horm.* **36**, 297–382.
- Morley, J. S. 1980 Structure–activity relationships of enkephalin-like peptides. *A. Rev. Pharmac. Toxicol.* **20**, 81–110.
- Niedel, J. E., Kahane, I. & Cuatrecasas, P. 1979 Receptor-mediated internalization of fluorescent chemotactic peptide by human neutrophils. *Science, Wash.* **205**, 1412–1414.
- Padlan, E. A., Cohen, G. H. & Davies, D. R. 1985 On the specificity of antibody/antigen interactions: phosphocholine binding to McPC 603 and the correlation of three-dimensional structure and sequence data. *Annls Inst. Pasteur, Paris* **136C**, 271–276, 293–294.
- Peabody, D. S., Ely, K. R. & Edmundson, A. B. 1980 Obligatory hybridization of heterologous immunoglobulin light chains into covalently linked dimers. *Biochemistry, Wash.* **19**, 2827–2834.
- Rossier, J., Audigier, Y., Ling, N., Cros, J. & Udenfriend, S. 1980 Met-enkephalin-Arg(6)-Phe(7), present in high amounts in brain of rat, cattle and man, is an opioid agonist. *Nature, Lond.* **288**, 88–90.
- Schiffer, M., Girling, R. L., Ely, K. R. & Edmundson, A. B. 1973 Structure of a λ -type Bence-Jones protein at 3.5 Å resolution. *Biochemistry, Wash.* **12**, 4620–4631.
- Schiffmann, E., Corcoran, B. A. & Wahl, S. M. 1975 *N*-formylmethionyl peptides as chemoattractants for leucocytes. *Proc. natn. Acad. Sci. U.S.A.* **72**, 1059–1062.
- Segal, D. M., Padlan, E. A., Cohen, G. H., Rudikoff, S., Potter, M. & Davies, D. R. 1974 The three-dimensional structure of a phosphorylcholine-binding mouse immunoglobulin Fab and the nature of the antigen-binding site. *Proc. natn. Acad. Sci. U.S.A.* **71**, 4298–4302.
- Sheriff, S., Silverton, E. W., Padlan, E. A., Cohen, G. H., Smith-Gill, S. J., Finzel, B. C. & Davies, D. R. 1987 Three-dimensional structure of an antibody–antigen complex. *Proc. natn. Acad. Sci. U.S.A.* **84**, 8075–8079.
- Showell, H. J., Freer, R. J., Zigmond, S. H., Schiffmann, E., Aswanikumar, S., Corcoran, B. A. & Becker, E. L. 1976 The structure–activity relations of synthetic peptides as chemotactic factors and inducers of lysosomal enzyme secretion for neutrophils. *J. exp. Med.* **143**, 1156–1169.
- Smith, R. G., Ballard, D. W., Blier, P. R., Pace, P. E., Bothwell, A. L. M., Herron, J. N., Edmundson, A. B. & Voss, E. W. Jr 1989 Structural features of a murine monoclonal anti-ssDNA autoantibody. *J. Indian Inst. Sci.* (In the press.)
- Snyder, S. H., Pert, C. B. & Pasternak, G. W. 1974 The opiate receptor. *Ann. intern. Med.* **81**, 534–540.
- Terenius, L. 1978 Endogenous peptides and analgesia. *A. Rev. Pharmac. Toxicol.* **18**, 189–204.
- Tulloch, P. A., Colman, P. M., Davis, P. C., Laver, W. G., Webster, R. G. & Air, G. M. 1986 Electron and X-ray diffraction studies of influenza neuraminidase complexed with monoclonal antibodies. *J. molec. Biol.* **190**, 215–225.

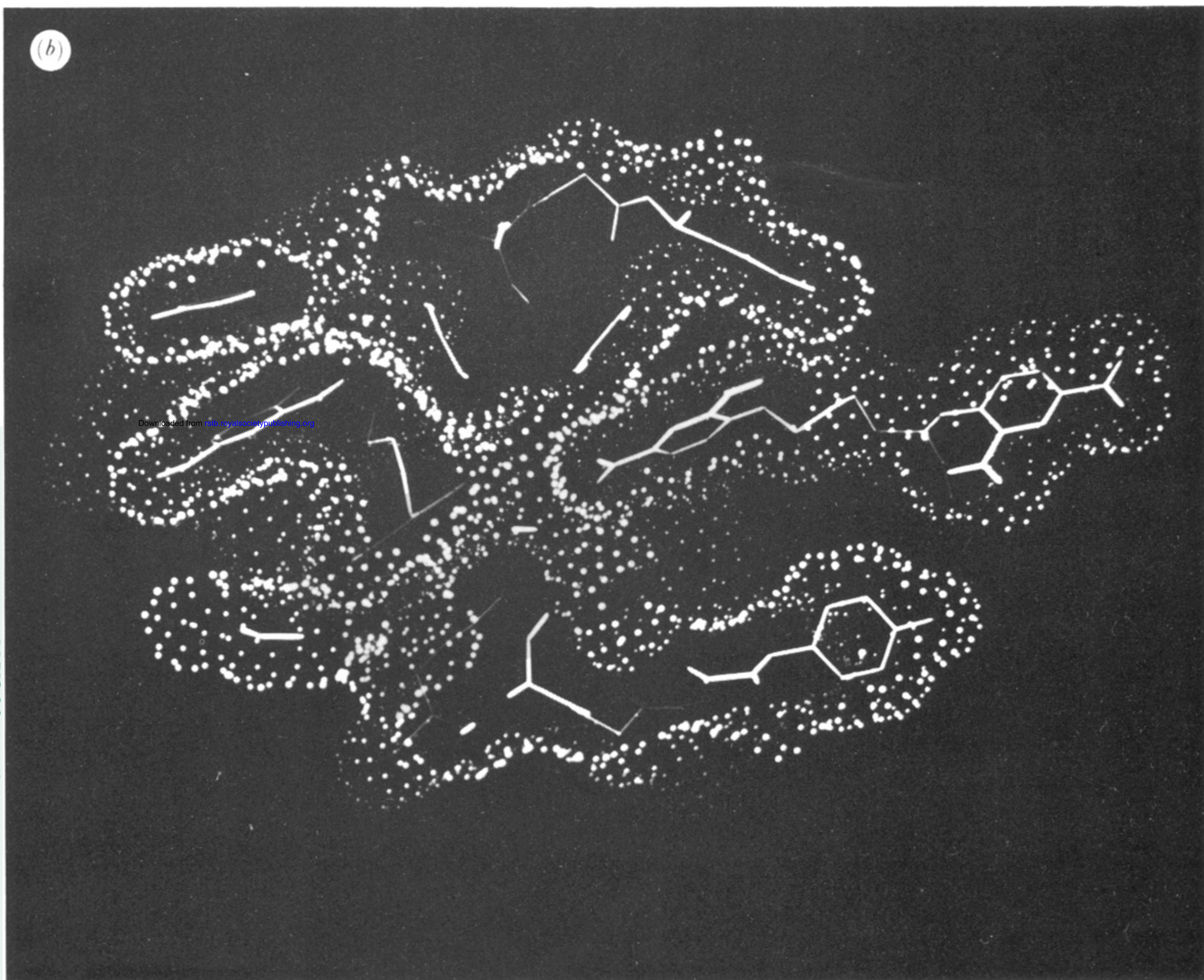
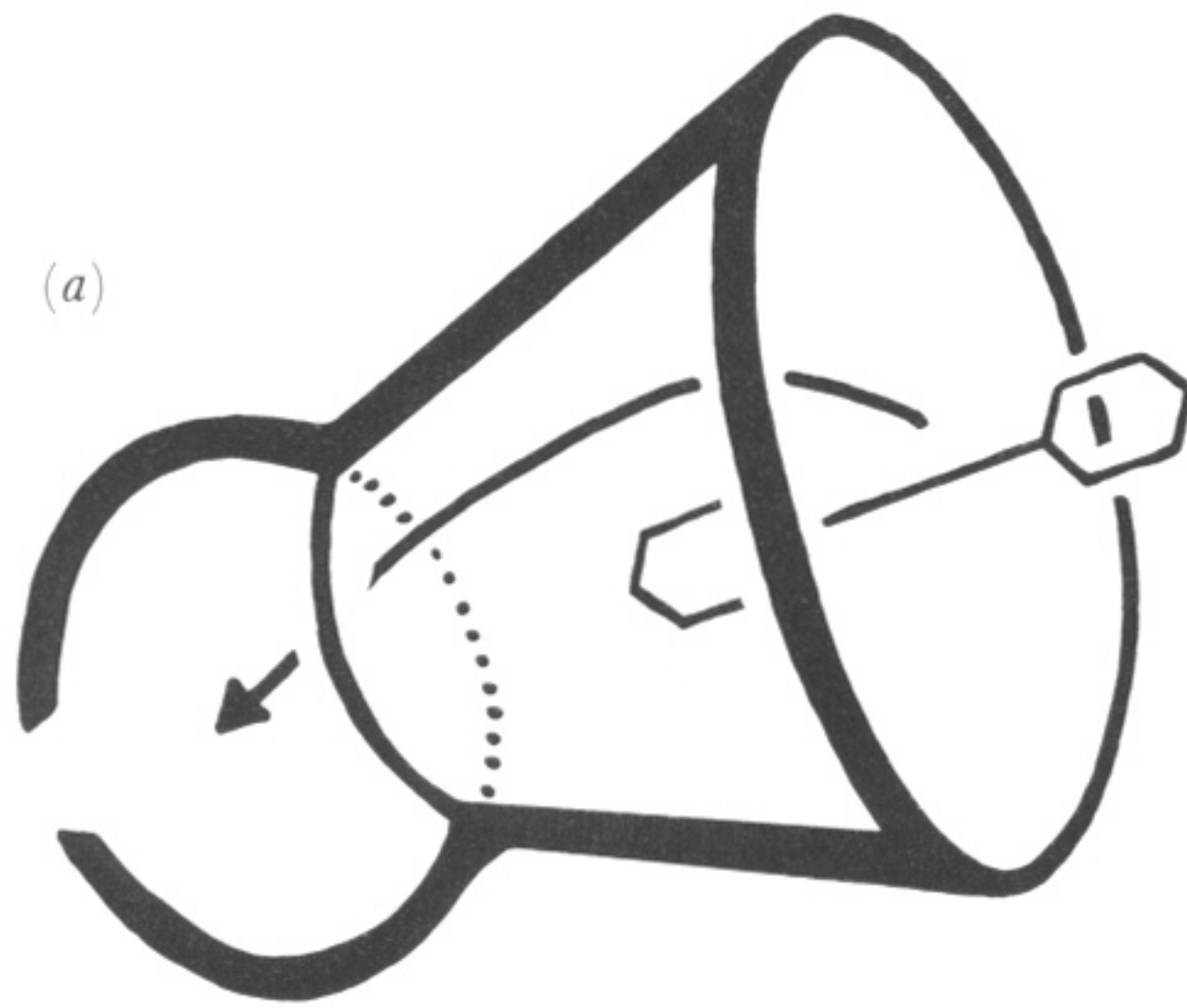


FIGURE 4. (a) Schematic view of the conical main cavity (right) and the ellipsoidal deep pocket (left). A model of bis(DNP)lysine is drawn in the approximate orientation observed in co-crystals of the ligand and protein. The arrow indicates a possible path to the deep pocket. (Drawing by Kathryn Ely.) (b) Surface dot representation (Connolly 1983) of the two tandemly bound molecules of bis(DNP)lysine in the main cavity (right) and deep pocket (left). This cutaway view was photographed directly from the screen of an Evans & Sutherland PS300 colour graphics system. The ligand molecule on the right is almost fully extended, and only one DNP ring is located inside the main cavity. This bis(DNP)lysine on the left is very compact and is completely enclosed in the deep pocket.